Analysis and characterization of complex reactor behaviour. A case study. [1]

Berit Floor Lund [a,b,*], Bjarne A. Foss [b], Kjell R. Løvåsen [c]

[a] *Sintef ICT, Applied Cybernetics, 7465 Trondheim, Norway*

[b] *Norwegian University of Science and Technology, NTNU, Institute of Engineering Cybernetics, 7491 Trondheim, Norway*

[c] *Elkem ASA, Silicon division, Kristiansand, Norway*

Abstract

This paper analyzes the steady state and dynamic behavior of a reactor for production of silicon metal, a submerged arc furnace. The furnace behavior has been analyzed through simulation studies using a detailed, industrially proven, mechanistic simulation model. The analysis reveals that the silicon furnace has changing and complex dynamic behaviour, including inverse responses and slow modes, especially close to optimality. The paper analyzes the causes of the changing dynamic behaviour. It also shows how the margins to optimality can be deduced from the dynamic response to changes in the carbon coverage input.

Key words: Reactor dynamic behavior, zero and pole drift, submerged arc silicon furnace

1 Introduction

Silicon metal is an important raw material for the chemical industry, for aluminium casting, and for the production of semiconductors in electronics and solar cells.

Silicon metal (Si) is produced from quartz (SiO_2) using carbon as the reduction material. The submerged arc silicon furnace is the heart of a silicon metal producing plant. The furnace is an endothermic chemical reactor with complex behaviour. The furnaces are mainly manually operated. This is a difficult task due to few on-line measurements, many disturbances, and multivariate and changing dynamic behaviour. Steady state operating conditions are seldom reached in an actual furnace.

This paper contributes to the understanding of the complex furnace behaviour by analysis of the steady state and dynamic behaviour. The analysis is based on simulation studies using the industrially proven model Simod, a proprietary model of Elkem ASA. The analysis was made possible through the development of a Matlab interface to the model.

The literature describing the causes of steady state sign change and changing dynamic behaviour in reactors and integrated process arrangements form

* Corresponding author. Tel. +47 594395; Fax +47 594399. E-mail address: berit.floor.lund@sintef.no (B. F. Lund)

Email addresses: baf@itk.ntnu.no (Bjarne A. Foss), kjell-ragnar.lovaasen@elkem.no (Kjell R. Løvåsen).

[1] This work has been supported by NTNU, Elkem ASA and SINTEF

the background of the analysis. Some aspects of silicon furnace behaviour are similar to those of for instance the van de Vusse example process. Kuhlmann and Bogle [4] examines the causes of the steady state sign change giving input multiplicity in a van de Vusse reactor. Kuhlmann and Bogle [4] point out that in some cases there exists a connection between models with input multiplicities and models with non-minimum phase behavior. Both characteristics are caused by competing physical effects on one output variable [2].

Drifting poles and zeros may also be caused by interconnections in process plants [6]. Morud and Skogestad [6] distinguish between external and internal interconnections. External interconnections are interconnections between subsystems associated with different processing equipment. Internal interconnections mean interconnections between phenomena within one process vessel. Within the internal interconnections, there exist recycling, parallel paths and series interconnections. Series interconnection is the simplest kind of interconnection and implies that there is a one-way flow between subsystems of material and/or energy. In a system with recycle, mass and/or energy flow is fed back in the process. Recycle generally moves the poles of the process. In most systems, recycle leads to positive feedback, according to Morud and Skogestad [6]. Parallel paths, or process "feed-forward", creates or moves the zeros of the process. If the effects of the parallel paths have opposite signs, they are competing effects which may give unstable zero dynamics, or inverse responses for linear systems. Jacobsen [3] points out that recycle also can move control

relevant zeros of a plant, and uses reactor and distillation column arrangement as an example.

The paper focuses on the steady state and dynamic responses to two critical inputs, carbon coverage and carbon reactivity. Effects of altering the electric power level have also been studied, but are not included in this paper.

Carbon coverage is the stoichiometric ratio of carbon to quartz in the feed. The precise definition of carbon coverage is provided in section 2 together with an overview over silicon metal production. The Simod model is presented in section 3. The steady state gain from carbon coverage to silicon tap-rate, i.e. the product production rate, is described in section 4.1. The steady state gain exhibits a sign change giving a steady state optimum [8]. Section 4.2 shows the underlying dynamic responses and quantifies the change in the dominant time constants. The possible causes of furnace behaviour are identified by analyzing the reaction chemistry of the silicon furnace, see section 4.3. The effect of variations in the carbon reactivity is described in section 5. Changes to the reactivity may be made deliberately by altering the carbon material composition (woodchips, coal and coke), or come as a result of unplanned changes in the composition or the carbon material properties. Section 6 contains the conclusion.

2 The submerged arc silicon furnace

The textbook by Schei et al. [8] gives an introduction to silicon metal chemistry and production. The heart of a silicon metal producing plant is the furnace, see figure 1. The raw materials, (SiO_2, C) are fed at the top and silicon metal *(Si)* is tapped at the bottom. The off-gases, mainly silicon oxide (SiO) and

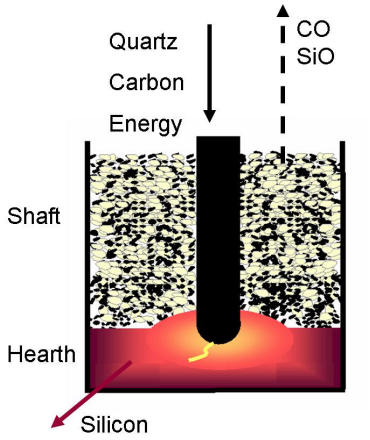

Fig. 1. Principal scetch of a silicon furnace

carbon monoxide (CO), oxidize at the furnace top and in the off-gas system. The oxidized SiO generates a microsilica dust [8] which is captured in a filter.

The required electrical energy supply relates to the physical dimensions of a furnace and determines the total mass conversion rate through the furnace. According to Schei et al. [8, chap 3.2.1], a typical medium-sized silicon furnace would be $20MW$, with a pot diameter of $7m$ and depth of $2.7m$.

The electric energy is supplied through consumable carbon electrodes. Approximately half of the energy is released through electric arcs in a gas filled

cavity formed in the lower part of the furnace around the electrode tips. This part of the furnace is referred to as *crater* or *hearth*. The rest of the electrical energy is supplied through ohmic conduction in the charge surrounding the cavity of the hearth and in the *shaft*, which is the upper, cooler part of the furnace.

The gross furnace reaction is written [8]

$$SiO_2{+}(1+x)C \rightarrow xSi + (1-x)SiO + (1+x)CO \tag{1}$$

where $x \in [0,1]$ is defined as the *silicon yield*, with a typical value of around 0.8. A yield of 1.0 can never be reached since some SiO always escapes at the furnace top. As can be seen from reaction (1), a higher silicon yield requires a higher fraction of carbon to the reaction. The required *carbon coverage* for a specified silicon yield, is defined by $\left(\frac{(1+x)}{2} \cdot 100\%\right)$.

In reality, a number of reactions take place in order for Si to be formed. The production of silicon oxide gas, SiO, is the engine of the furnace reaction chemistry. Since SiO_2 is a very stable chemical component, the formation of SiO gas is a highly endothermic reaction between silicon metal and molten SiO_2,

$$Si + SiO_2 \rightleftharpoons 2SiO \tag{2}$$

The reaction mainly takes place in the hearth. Some of the SiO is consumed

within the hearth to form silicon metal according to the reaction,

$$SiC + SiO \rightarrow 2Si + CO \tag{3}$$

Most of the SiC required in the reaction (3) is formed in the shaft in an exothermic reaction between SiO rising from the hearth, and the carbon feed in the shaft,

$$SiO + 2C \rightarrow SiC + CO \tag{4}$$

SiC is a solid, and travels down to the hearth where it is consumed to produce silicon according to reaction (3). Reaction (4) also takes place in the hearth if unreacted carbon reaches the hearth. If the production of SiC by (3) is larger than the consumption by (4), SiC accumulates in the hearth, giving an *over-coked* operating condition. The furnace is normally run under *under-coked* conditions, where all the generated SiC is consumed.

The *carbon reactivity*, r, is the reaction rate constant for (4). Typical values lie between 0.3 and 0.7.

Some of the SiO gas rising up through the shaft condenses, and travels down with the other solids to the hearth as $Si{\cdot}SiO_2$ condensate. The transportation and condensation of SiO is the main source of heating of the shaft. In the hearth, the condensate splits into Si and SiO_2 again.

The reactions (2)-(4) are the dominant reactions under normal operating con-

ditions. Other reactions dominate when the SiO partial pressure is lower [8], for instance during start-up.

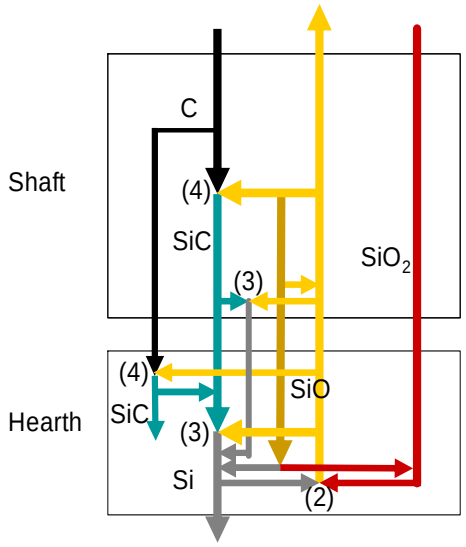

Fig. 2. Component flows between shaft and hearth reactions.

Figure 2 illustrates the flows of components between reactions in the furnace is illustrated. The component flows are illustrated with arrows of different color, and the chemical reactions (2)-(4) take place where the arrows meet.

3 The Simod model

The Simod model described in Foss and Wasbø [1] is a nonlinear, dynamic representation of the mass balances, chemical reactions and thermodynamic behavior a submerged arc silicon furnace. The Simod model has been written in a Differential Algebraic Equation (DAE) form. The model is one-dimensional, which means that no gradients are assumed in the horizontal direction.

The distributed nature of the process and the model has been approached

using finite volumes, each with homogeneous conditions, and flows of energy and mass between them. The hearth is considered as one volume that can vary in height. The shaft can be divided into a number of compartments, typically ten. The top shaft volume can vary in height to represent variations in charging.

The main mass transportation mechanisms in the furnace and model are the downward transportation of solid and liquid phase materials, and the upward transportation of gas phase components. The dynamics of the gas, liquid and solid phases have a large span in time constants resulting in a very stiff model. The stiffness problem is handled by ignoring the gas dynamics and converting the corresponding dynamic equations into an algebraic equations. The algebraic equations of the model are computed prior to the integration of the dominant solid state dynamics which is then solved by a numerical integration scheme for non-stiff systems.

The feeding and tapping operations in real furnaces have been simulated in the model using discrete on-off controllers with dead-bands specified by the user. The feed and tap-rate can alternatively be set through model inputs.

The model can be parametrized to represent furnaces of different physical dimension. The thermochemical data used in the model is provided by a commercial software package.

The model itself, the solution scheme for the algebraic equations and the

integration scheme for the dynamic part of the model have proven efficient and robust through more than 5 years of use. Extensive work has been undertaken by Elkem personnel to verify the model's behavior. The model has been an important tool for process specialists for analysis of the process. Further, the model has also been used in operator training.

4 Carbon coverage to silicon tap-rate response

In section 4.1 the steady state gain from carbon coverage to silicon tap-rate is shown. The net dynamic responses to perturbations in the carbon coverage are described in section 4.2 and the changes in the dominant time constants are quantified. The possible causes of the changing dynamic behaviour are analyzed in section 4.3.

All simulations in this section have been made with typical values for a medium size reactor with an electric power input of 22 MW, and carbon reactivity $r = 0.56$.

4.1 Steady state gain

The carbon coverage input has been simulated to steady state for the carbon coverage $90 \ldots 96\%$. The steady state gain for carbon coverage to silicon tap-rate is plotted in figure 3. The steady state gain is relatively constant up to

96%. Above 96.5%, silicon carbide starts to accumulate in the hearth. This would cause severe tapping problems in the furnace. In the simulator, ideal tapping is assumed, but the build-up of silicon carbide gives a higher hearth

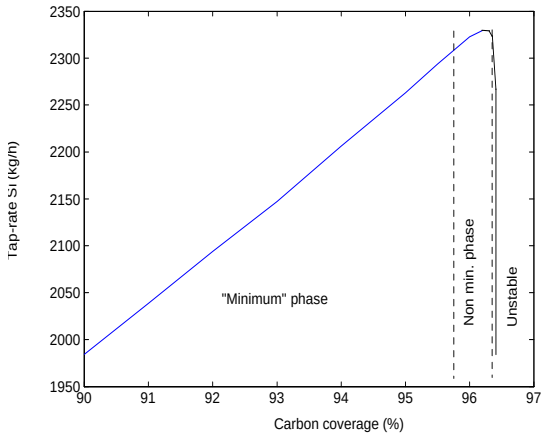

Fig. 3. Steady state gain from carbon coverage (%) to silicon tap-rate (kg/h).

and a shallower shaft, causing a sign change in the gain, and a negative integrating effect on the tap-rate. This is indicated by a vertical gain curve above 96.5% in figure 3, and the region above 96.5% is in this sense unstable.

The maximal carbon coverage rate one can use and still be in the under-coked operating region, is referred to as "optimal carbon coverage". Above this carbon coverage rate, the furnace will be over-coked. The optimal gross carbon coverage rate lies at approximately 96.5% for these simulations. The region around 96% is denoted "non-minimum phase". This will be further explained later.

The steady state gain curve shown in figure 3 has the sign change in common with a process with input multiplicities. Since silicon carbide accumulates in the hearth, however, there is a negative integrating effect for large inputs, and

no steady state value for the gain exists at this side of the optimum.

4.2 Dynamic responses to carbon coverage changes

In order to explain the change in the steady state gain around optimal carbon coverage, the dynamic behavior depending on carbon coverage level is analyzed.

The net step response at each carbon coverage level has been found by adding a small positive step of 0.1% carbon coverage at time 1 hours, and subtracting the steady state silicon tap-rate from each response so that a net response, starting from zero, is obtained. The resulting responses can then be compared, see figure 4. Figure 4 shows that the dominant time constant increases for increasing levels of carbon coverage. For 96% carbon coverage there is an inverse response, and a very slow positive response. At 97% carbon coverage

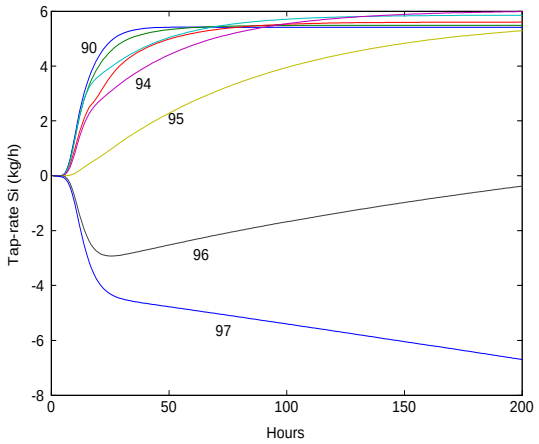

Fig. 4. Net step responses in tap-rate Si to a 0.1% step in the carbon coverage at carbon coverage values 90 . . . 97%.

the gain is negative, and no steady state value is reached.

The change in the dominant dynamic behavior can also be observed in the silica fume production. Figure 5 shows silica fume responses corresponding to figure 4. The main difference between figure 5 and 4, in addition to the negative gain, is that the inverse response observed in 4 is not present in 5, and it is therefore not so easy to determine from the silica fume rate when over-coking is reached.

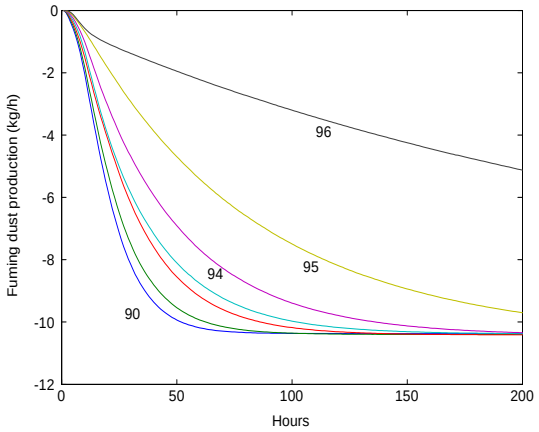

Fig. 5. Step response to carbon coverage in silica fume production. $r = 0.56$.

In the following, an explanation of the changing dynamic behavior is sought. Figure 2 indicates that several types of mechanisms may be involved, and the conversion rates of the furnace reactions are quantified in the following.

4.2.1 Quantification changes in dominant time constants

A third order transfer function has proven to give a sufficient approximation to the responses shown in figure 4:

$$H(s) = \frac{K_1 e^{-\tau s}(1 + T_1 s)}{(1 + T_2 s)(1 + T_3 s)(1 + T_4 s)} \tag{5}$$

The transport delay and time constants in (5) where identified using the Matlab script "lsqcurvefit". This revealed that the dynamic behavior was dominated by a zero and a pole, whose time constants T_1 and T_2 have been plotted against the carbon coverage level in figure 6. The pole and zero cancel each other for 90% carbon coverage. As the carbon coverage increases, the time constant of the pole increases, whereas the time constant of the zero decreases and finally goes negative.

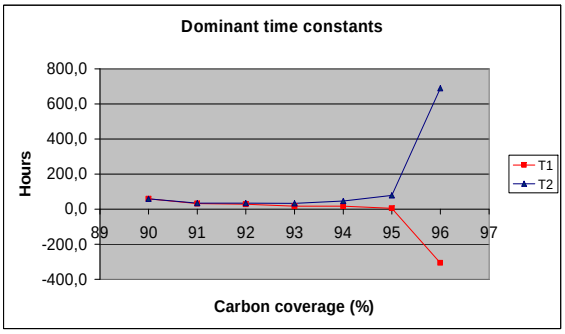

Fig. 6. Development of the dominant time constants T_1 and T_2 for increasing carbon coverage.

4.3 Analysis of reaction conversion rates

In order to explain the changes in the dynamic behavior, the conversion rates of the reactions (2), (3), and (4) were quantified for different carbon coverage levels.

The upper curve in figure 7 shows the steady state conversion rate of the SiO producing reaction (2) and the lower the Si producing reaction (3) in the hearth. The production of SiO is $2 \times 88\ kmol/h = 176 kmol/h$ at 90% carbon

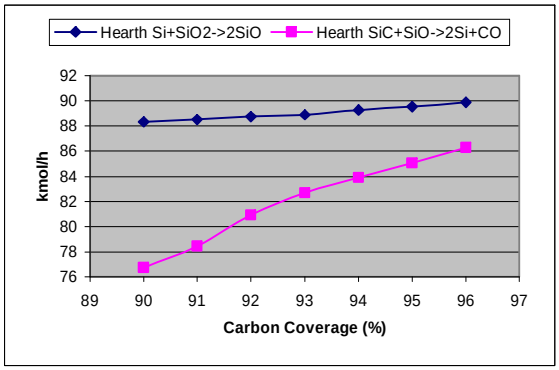

Fig. 7. Steady state conversion rates for SiO and Si producing reactions in hearth.

coverage, and $2 \times 90 kmol/h = 180 kmol/h$ at 96% carbon coverage. This gives an increase in the SiO production of $4 kmol/h$. The increased consumption of SiO, by the lower curve, is almost $10 kmol/h$. Since the SiO consumption in the hearth increases more than the production, the SiO level in the shaft will be lower for higher carbon coverage levels.

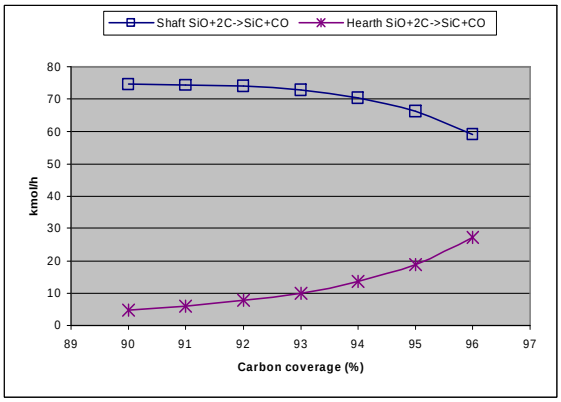

Fig. 8. SiC generation in the shaft (upper) and hearth (lower).

Figure 8 shows the conversion rates for reaction (4) in the shaft (upper) and hearth (lower). For low carbon coverage rates, most of the SiC is formed in the shaft and little in the hearth. For higher carbon coverage rates less SiC is formed in the shaft and more in the hearth. This can be explained by the increased SiO consumption in the hearth due to increased production of Si,

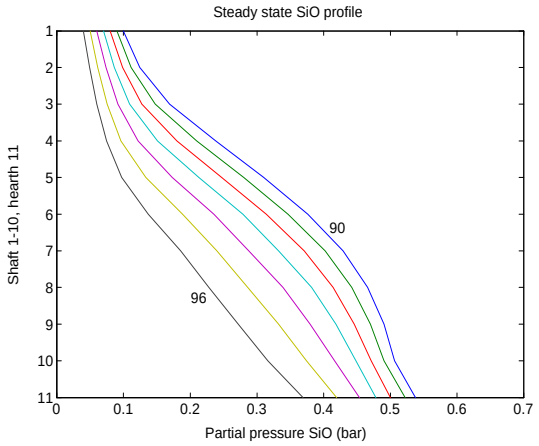

Fig. 9. Steady state SiO profile for carbon coverage values $90 \ldots 96\%$. Element 1 on the vertical axis corresponds to the shaft top, element 11 to the hearth.

as seen in figure 7. In addition, the increased production of SiC in the hearth reduces the SiO in the shaft further, see figure 9.

The steady state SiC profile down through the furnace is shown in figure 10. The amount of SiC in the hearth increases more close to optimal carbon coverage.

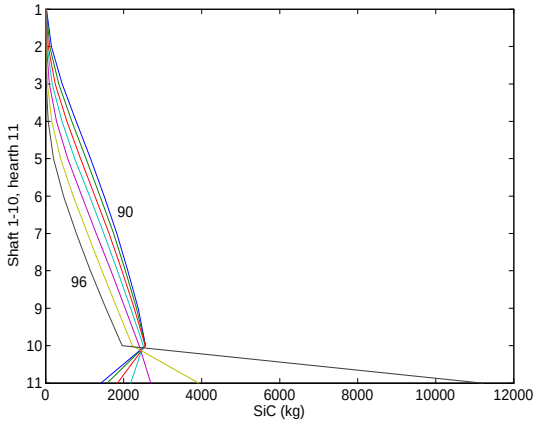

Fig. 10. Steady state SiC profile for carbon coverage $90 \ldots 96\%$. Element 1 on the vertical axis corresponds to the shaft top, element 11 to the hearth.

4.4 Resulting reaction patterns

By ignoring the recycling of SiO through condensation in the shaft, figure 2 can be redrawn emphasizing the response from carbon to tapped silicon, represented by figures 11 and 12. The shaft reactions are to the left of the dashed line, the hearth reactions to the right. Both figures illustrate the recycling of silicon through the reaction with SiO_2 in the hearth. Figure 11 shows the main reactions when the furnace is run under-coked, and with carbon coverage far below the optimal carbon coverage value.

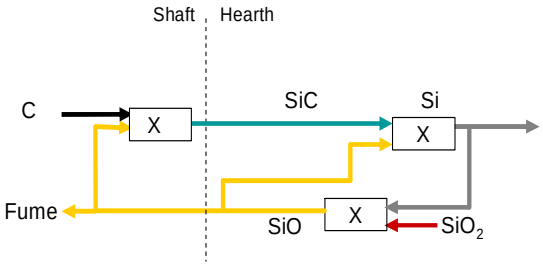

Fig. 11. Component flows and reactions when carbon coverage is far below optimal value in the under-coked region.

Figure 12 shows the component flows and reactions with a carbon coverage close to or at the optimum value, but not over-coked. In this case some unreacted carbon enters the hearth, and SiC is also formed in the hearth, indicated by the top, middle reaction.

In this situation, the carbon to silicon tap-rate response exhibits an inverse response, according to figure 4. Figure 12 clearly illustrates that the SiC and Si production in the hearth compete for SiO in the hearth. The SiC production in the hearth is therefore a candidate for explaining the inverse response at

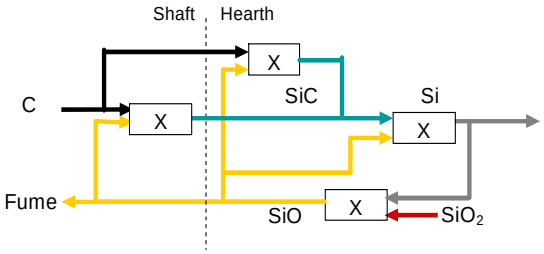

Fig. 12. Component flows and reactions in the hearth and shaft at close to optimal carbon coverage, still in the under-coked region.

high carbon coverage values.

One possible reason for the slower response, i.e. the large time constant in the dominant pole, at high carbon coverage levels, is that the carbon in the hearth needs time to react to SiC, whereas for low carbon coverage values, the SiC is formed in the shaft and comes down to the hearth "ready" to enter the Si producing reaction. Another possible reason for the slower response at high carbon coverage rates is the decreased amount of SiO gas in the furnace, see the steady state profiles for SiO in figure 9. Since the partial pressure of SiO (above an equilibrium pressure) drives the SiC and Si generating reactions, less free SiO in the furnace will clearly give a slower response in all reactions. It is also possible that the high production of SiC in the hearth also affects the time constant of the pole.

5 Impact of carbon reactivity variations

In the previous section, the effect of carbon coverage variations was analyzed, keeping the carbon reactivity constant. In this section, the steady state and

dynamic effects of changes in the carbon reactivity are studied.

The carbon reactivity parameter in the model gives a lumped representation of several physical properties of the carbon materials, such as the relative mix of carbon materials (wood-chips, coal and coke), porosity, and the size distribution and other properties. Changes in the carbon reactivity may be made deliberately by changing the carbon material mix, or come as a disturbance. The off-line determination of actual, effective carbon reactivity is also associated with some uncertainty [7].

All simulations have been made using $22MW$ as the power input.

5.1 Steady state effect of carbon reactivity variations

Figure 13 shows the steady state gain curves from carbon coverage to silicon tap-rate for reactivity values $r = 0.3 \ldots 0.7$.

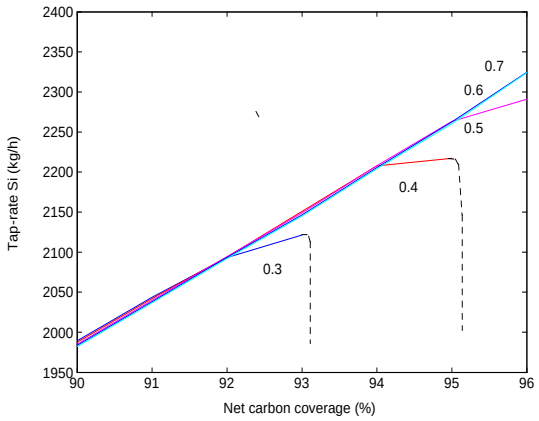

Fig. 13. Steady state gain from carbon coverage to silicon tap-rate for $r = 0.3 \ldots 0.7$.

The figure shows that over-coking occurs around 93% carbon coverage for

$r = 0.3$ whereas for $r = 0.4$, over-coking occurs above 95%. A higher carbon reactivity therefore gives a higher maximum achievable silicon production.

One can also observe that at 91% carbon coverage, which is far away from over-coking for all reactivity values, the steady state tap-rate is the same. This means that the steady state gain is relatively independent of the reactivity except at optimality.

The steady state silicon yield versus carbon coverage for different reactivity values is shown in figure 14. The silicon yield is the ratio of silicon recovered as tapped metal, relative to the silicon supplied as quartz. The figure basically shows the same as figure 13, that higher yield can be reached using higher reactivity carbon.

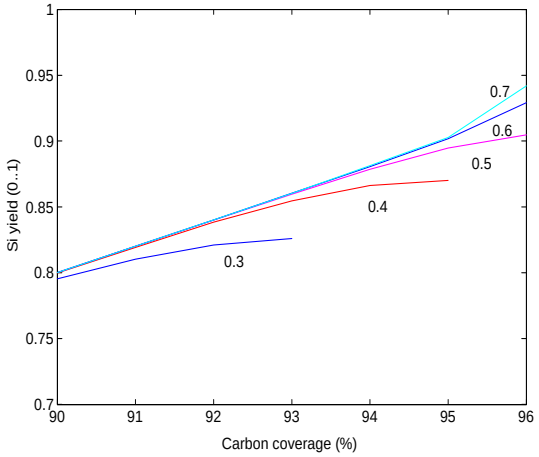

Fig. 14. Silicon yield vs. carbon coverage for carbon reactivities $r = 0.3 \ldots 0.7$.

In figure 15 the carbon coverage has been perturbed at 91% carbon coverage for different reactivities. The response for the highest reactivity is fast, and contains a small overshoot, whereas for the lowest reactivity the slow step

response starts with a small inverse. This indicates that the inverse response and slow pole observed for higher carbon coverage values for $r = 0.56$ in figure 4 occurs at lower carbon coverage values for lower reactivity values.

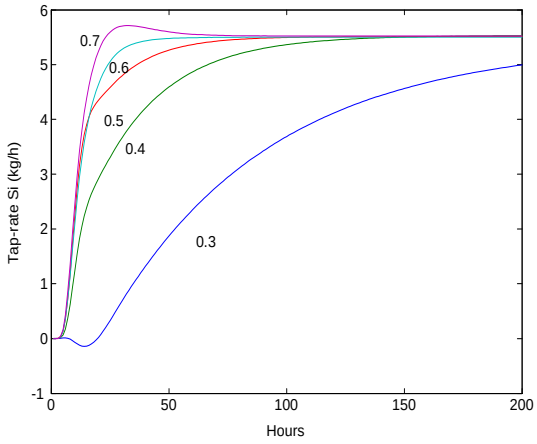

Fig. 15. Net step responses in silicon tap-rate to a 0.1% step in carbon coverage at 91% for reactivities $r = 0.3 \ldots 0.7$.

To investigate this further, the carbon coverage has been perturbed for a high reactivity, $r = 0.7$, and the net step responses for all carbon coverage levels have been plotted in figure 16. Figure 16 shows a fast response with overshoot for carbon coverage values 90% and 91%. The response at 96% is relatively slow, but there is no significant inverse response for $r = 0.7$.

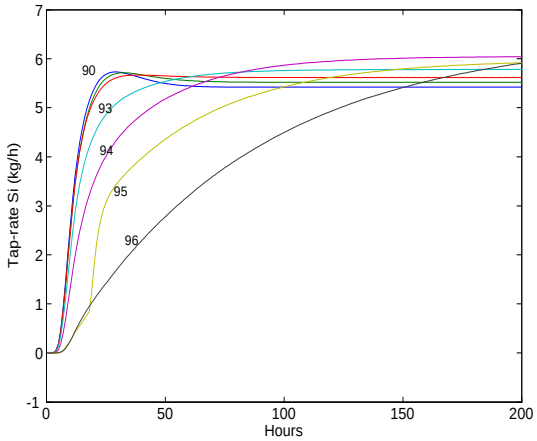

Fig. 16. Net step response in silicon tap-rate to 0.1% step in carbon coverage at carbon reactivity $r = 0.7$.

Figures 15, 16, and 4 show that a furnace operating far below the maximum carbon coverage for a particular carbon reactivity value, will have a fast carbon coverage to tap-rate response. A furnace operated at the optimum will have a much slower response. The dominant dynamics of the furnace is therefore an indication of the margins to optimality for the furnace, regardless of where the carbon reactivity places the optimal operating point.

6 Conclusion

The paper contributes to the understanding of the complex behaviour of the chemical reactor used for silicon metal production. An important characteristic of silicon furnace behaviour is a sign change in the steady state gain giving a production optimum. The paper has described how the dynamic behaviour of the furnace changes, especially close to optimum. The causes of these changes are sought in the chemical reactions patters of the furnace. The analysis shows that increased amount of carbon in the lower part of the furnace has a profound impact on the furnace dynamics around optimum.

The paper has also described how the dynamic response from carbon coverage to silicon tap-rate is an indication of the margins to the optimal operating point for a given carbon reactivity. These results have been verified qualitatively by process specialists in Elkem ASA. Since there are uncertainties linked to determining the effective carbon reactivity, and also since there may be dis-

turbances in the carbon material mix, there is often uncertainty connected to the location of the furnace optimum. Determining the optimal carbon coverage level is therefore one of the most important challenges in furnace operation. The paper has shown that the dominant time constants of the furnace indicate the margins to optimality regardless of carbon reactivity value. A fast response to a carbon coverage perturbation is an indication that the carbon coverage can be increased significantly, whereas a slow response indicate that the margins to over-coking are small. This insight may be implemented during operation by perturbing the carbon coverage level more or less continuously in operation. Finally, the paper has shown that the changes in dominant dynamic behaviour of the furnace can be observed both through the silicon tap-rate as well as the silica dust production.

References

[1] B. A. Foss and S. O. Wasbø. An integration scheme for stiff solid-gas reactor models. *Computer Methods in Applied Mechanics and Engineering*, 190/45:6009–6021, 2001.

[2] E. W. Jacobsen. Dynamics of systems with steady state input multiplicity. *Presented at AiChE Annual Meeting, San Fransisco*, 1994.

[3] E. W. Jacobsen. On the dynamics of integrated plants - non-minimum phase behavior. *Journal of Process Control*, 9:439–451, 1999.

[4] A. Kuhlmann and D. Bogle. Study on nonminimum phase behavious and

optimal operation. *Computers Chem. Engineering*, 21:397–402, 1997.

[5] B. F. Lund, B. A. Foss, K. R. Løvåsen, and B. E. Ydstie. System analysis of complex reactor behavior - a case study. In *Proceedings of DYCOPS 7*. IFAC, 2004.

[6] J. Morud and S. Skogestad. Dynamic behaviour of integrated plants. *Journal of Process Control*, 6(2/3):145–156, 1996.

[7] E. H. Myrhaug. *Non-Fossil Reduction Materials in the Silicon Process - Properties and Behaviour*. PhD thesis, NTNU, 2003.

[8] A. Schei, J. K. Tuset, and H. Tveit. *Production of High Silicon Alloys*. Tapir forlag, Trondheim, Norway, 1998.